

Mitigation of Silver Ion Loss from Solution by Polymer Coating of Metal Surfaces, Part IV

John Vance¹

KBRwyle, NASA Ames Research Center, Moffett Field, CA 94035

and

Lance Delzeit²

NASA Ames Research Center, Moffett Field, CA 94035

Ionic silver (Ag^+) biocide is a leading candidate to provide residual microbial control in spacecraft potable water systems, but suffers from rapid concentration loss due to interactions with the metallic storage containers and tubing. One approach to resolve this problem is the coating of metal surfaces with an inert barrier film. In previous reports, we have described our investigations addressing Ag^+ loss mitigation and adhesion performance of parylene barrier coatings on coupons of several metal alloys and 316L tubing under static immersion. In such conditions, parylene-C and -AF4 coatings have shown excellent Ag^+ loss mitigation and mixed long-term adhesion performance, depending on parylene species and substrate surface chemistry/structure. In Part IV of this series, we report on our work to investigate the performance of parylene-C barrier coatings, under more challenging and realistic conditions, in order to evaluate potential suitability for use. The resilience and associated Ag^+ loss with Parylene-C coating on $\frac{1}{2}$ " (12.7 mm) 316L tubing and fittings under medium-term immersion and repeated fitting dis/reassembly were investigated. Potential mechanical challenges to barrier coatings in spacecraft potable water systems were investigated, with two main focuses being identified: liquid flow/pressure cycling in tubing and cyclic operation of bellows in positive-expulsion storage tanks. Two corresponding testbeds for experimental characterization of coating performance were developed. In the Flow/Pressure Testbed System, Ag^+ solution will be pumped through internally coated 316L tubing, with optional pressure cycling. In the Bellows Tank Testbed System, an internally coated edge-welded 316L bellows containing Ag^+ solution will be cyclically extended and compressed, analogous to the operation of bellows tanks used for potable water storage and delivery on the International Space Station. The design and operation of these testbeds are described. Finally, the Ag^+ adsorption and saturation behaviors of Kalrez and Viton, for potential use as seal materials in fittings and other connections, were characterized in limited experiments.

Nomenclature

316L	=	austenitic Fe-Cr-Ni-Mo stainless steel (low-carbon grade)
AdPro Plus™	=	AdPro Plus™ proprietary adhesion promoter (Specialty Coating Systems, Inc.)
Ag^+	=	silver(I) ion
AgF	=	silver(I) fluoride
AN	=	Army-Navy
A/V	=	surface area/volume ratio
cm^{-1}	=	cm^2/cm^3
COTS	=	commercial-off-the-shelf
I.D.	=	inner diameter
kPa	=	kilopascal
mL	=	milliliter

¹ Research Engineer, Bioengineering Branch, NASA ARC N239-15, Moffett Field, CA 94035.

² Physical Scientist, Bioengineering Branch, NASA ARC N239-15, Moffett Field, CA 94035.

<i>mm</i>	=	millimeter
<i>O.D.</i>	=	outer diameter
<i>psi</i>	=	pound per square inch
<i>PTFE</i>	=	polytetrafluoroethylene
μg	=	microgram
μm	=	micrometer
<i>NaF</i>	=	sodium fluoride
<i>parylene-C</i>	=	poly(chloro-p-xylylene)
<i>parylene</i>	=	poly(p-xylylene) polymers
<i>ppb</i>	=	parts per billion (mass)
<i>SCS</i>	=	Specialty Coating Systems, Inc.

I. Introduction

NASA has identified ionic silver (Ag^+) as a promising candidate biocide for spacecraft potable water systems in future exploration-class missions. Unfortunately, Ag^+ in solution is known to react with metal surfaces, resulting in rapid concentration depletion and potential loss of microbial control. This behavior has motivated interest in mitigation techniques such as coating of wetted surfaces with inert barrier coatings or replacement of passive metal alloys with alternative materials such as engineering-grade thermoplastics.¹ Most early stage work investigating Ag^+ compatibility has focused on static soak testing, which is straightforward and can provide relatively conclusive results regarding the suitability of robust bulk materials. In the case of barrier coatings, however, more rigorous testing is required to predict performance in real-world application. During system assembly or working service various forms of degradation may potentially occur leading to coating sloughing or metal exposure, resulting in Ag^+ loss. Small area-fraction exposure can result in significant to near-total loss of Ag^+ to the metal within the local vicinity and failure of biocidal control, with particular risk during extended system dormancy, as the length-scale of diffusion increases with the square root of time. It is therefore necessary to demonstrate adequate resilience if life support system designers are to be confident in specifying a given coating.

Given our success with coated metal coupons and tubing with fittings in static soak tests in previous work (particularly with parylene-C),^{2-4*} it naturally followed that the performance of these coatings under more representative (and challenging) conditions should be investigated. Upon examining the design of the potable water system in service on the ISS and considering likely requirements of future exploration-class systems, two focus areas identified. We then designed corresponding testbed systems to investigate coating performance in practical experiments. These are described briefly below, and then in detail in later sections.

The first combines pressure cycling and water flow, which is most deleterious in narrow (high velocity flow) paths such as those in tubing or valves. Shear, turbulent, and impinging flow may cause significant surface erosion, while pressure cycling may deleteriously affect adhesion to the metal substrate or result in bulk (fatigue-based) failure of the coating. We chose a pressure cycle range of 0 to 30 psig (similar to maximum pressure found in the ISS Potable Water Bus (PWB))⁷ and a nominal flow rate of 100 ml/minute (typical flow rate from the ISS Water Processor Assembly (WPA))⁸ as appropriate challenges. In order to characterize the performance of parylene-C under flow, pressure, and combined challenges, we designed and built a Flow/Pressure Testbed System that will be used to characterize the performance of internally-coated 316L tubing.

The second is repeated deformational cycling of critical mechanical components, most significantly in the operation of edge-welded bellows tanks, such as those found in the ISS Potable Water Storage and Delivery ORUs in the PWB. These may present some of the greatest challenges to soft polymer barrier coatings, with significant surface strain, risk of film pulverization at the welds, and design life requirements of up to 10,000s of expansion/contraction cycles. After surveying the geometries of commercially available edge-welded bellows, we designed a semi-custom 316L bellows assembly with manufacturer Duraflex, Inc. The diaphragm geometry of the bellows selected was the most representative to bellows used in the ISS Potable Water System readily available. This assembly forms the core of the bellows tank, and is cycled by modulating the differential pressure across the wet and dry sides of the bellows, using an electro-pneumatic drive system. Parylene-C performance in coated bellows subject to cycling will be

*This work features material adapted from a previous publication⁴ and reports to NASA Advanced Exploration Systems-Habitation Systems Project management^{5,6}

characterized with Ag^+ loss experiments and visual inspection. Preliminary operation has confirmed functionality of the Bellows Testbed.

In a previous work,⁴ we completed a preliminary investigation into the performance of parylene-C coatings with three different types of 316L tube/fitting systems: 37° Army-Navy (AN) flare fittings (standard in spacecraft water systems), Swagelok VCO™ O-ring face seal fittings, and tri-clamp gasket sanitary fittings. Here, we continue that work, characterizing performance with Ag^+ loss determinations and macrophotography of coating damage during medium-term immersion experiments with multiple fitting assembly/disassembly cycles. Such a challenge corresponds to initial assembly of a fluid connection and then replacement of a component, as in an ORU. We also completed limited experiments concerning the Ag^+ loss and saturation behavior of Kalrez and Viton, which could be useful as seal materials in the above fittings and for other fluidic connections.

II. The Flow/Pressure Cycling Testbed System

A. Background and General System Description

The Flow/Pressure Testbed System is a recirculating water flow system driven with a peristaltic pump (Masterflex L/S Digital Drive, with L/S Standard Pump Heads and Tygon Chemical pump tubing, 1/4" (6.4 mm) I.D. x 3/8" (9.5 mm) O.D.). A basic schematic of the system is reproduced in Figure 1a, and a photograph of the system with test specimens is shown in Figure 1b. The liquid reservoir and filter are covered with Al foil to minimize photoreaction of the Ag^+ . The system is constructed with inert polymers in the wetted flow path, in order to more selectively probe Ag^+ loss to the coated test specimens. The section of the testbed with the test specimens can be pressurized using a removable polysulfone orifice in series; by adjusting the orifice diameter and flow rate, a range of backpressures can be generated. The Ag^+ solution flows from the pump, through the test specimens, passes through a filter, the orifice, and into a reservoir, which then feeds the pump. Pressure cycling is done by intermittently stopping the peristaltic pump (and system flow) using its built-in computer control system, removing the backpressure generated by the orifice. The test articles are pre-fabricated 316L sanitary spools and 90° elbows (0.50" (12.7 mm) O.D., 0.37" (9.4 mm) I.D.) internally coated with a nominal 25 μm of parylene-C and are connected into the flow loop with sanitary-to-barb adapter fittings. Four pairs (spool and elbow) of test articles are connected to the flow system in series. These can also be removed from the testbed for high A/V static Ag^+ loss testing. The testbed is then free for an alternate set of test articles while the first undergoes static testing.

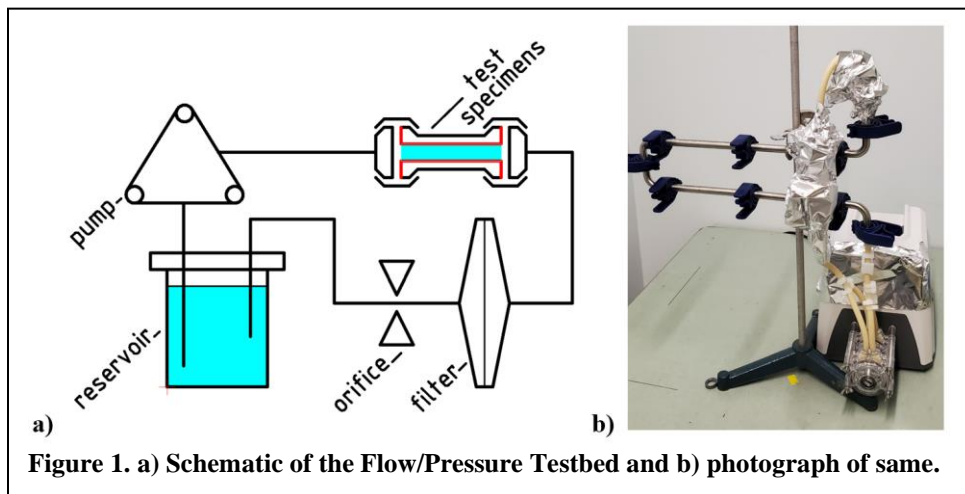


Figure 1. a) Schematic of the Flow/Pressure Testbed and b) photograph of same.

B. Preliminary Operation and Functional Checks

Preliminary operation of the system showed that operation at elevated pressure (with the flow-restricting orifice) resulted in accelerated damage to the multi-layer Tygon Chemical™ peristaltic tubing, which has been found to be highly inert to Ag^+ in static tests by us and others,⁹ in the pump heads, and weekly replacement of those sections of tubing is expected to be required. During, control runs excluding the test specimens, near total loss of Ag^+ was observed, along with a reddish-brown precipitate or reaction product on the polypropylene membrane employed in the filter, as shown in Figure 2. In tests where the filter was used, it is unclear the product is carried to the filter membrane, or if the Ag^+ is reacting with the highly-porous polypropylene membrane. A large loss was also observed

in experiments in which the filter was excluded, suggesting that other Ag^+ sinks are active. The other materials employed in the testbed, PVDF and polypropylene, have been found to be well compatible with Ag^+ .^{1,9}

It is unclear if a reaction producing an insoluble product is

occurring in the liquid bulk at the inner walls of the Tygon Chemical™ tubing or thermoplastic fittings. Pump operation may be damaging the inert inner layer of the Tygon Chemical tubing, potentially exposing a more reactive surface. Alternatively, constant liquid flow and consequent oxygenation of the Ag^+ solution may be accelerating loss kinetics. After resolving these issues with further control experiments and potential design modifications, we will begin operation of the testbed system with coated 316L specimens and uncoated control specimens.

III. The Bellows Tank Testbed System

A. Background

The Bellows Tank Testbed System (Bellows Testbed) is a sub-scale analog of the bellows tanks found in the ISS Potable Water Storage and Delivery ORUs that follow the Water Processor Assembly (WPA). Those tanks are internally wetted, with expulsion of the potable water driven by gas pressurant on the dry side of the bellows, with the differential pressure (dry side - wet side) increasing as the tank is emptied and the bellows compresses. The pressure at the liquid side of the bellows ranges between ~15-30 psi (100-200 kPa) in the Delivery Tank, which provides fully pressurized water to the Potable Water Dispenser, with a lower range in the Storage Tank, which receives water processed by the WPA.¹⁰ Water is pumped by a gear pump from the large volume, low pressure Storage Tank to the smaller volume, high pressure Delivery tank. These bellows are constructed out of edge-welded 316L stainless steel diaphragms, with design life in the 10,000s of cycles. Metal bellows tanks are used in the ISS potable water system due to (among other reasons) long service life, positive expulsion in microgravity, and negligible gas permeation. It is worth noting that the convoluted geometry of edge-welded bellows would increase the surface area of metal that would be exposed to Ag^+ -bearing potable water by approximately an order of magnitude vs. a cylindrical tank of similar dimensions, although diffusional limitations may help moderate Ag^+ loss in the bulk of the water.

As described in the introduction, the repeated mechanical action of the bellows tanks poses particular difficulty for the successful application of barrier coatings for Ag^+ loss mitigation. In the course of this survey we identified an alternative nested convolute bellows design (produced by hydroforming) introduced by the former Gardner Bellows Corporation (acquired by Duraflex, Inc.).¹¹ This may be of future interest if the geometry of edge-welded bellows proves unsuitable to barrier coatings, as it removes the small radius geometry at the edge welds between (bellows) diaphragms (potentially eliminating pulverization and cracking of the coating). Unfortunately, this type of bellows is no longer in regular production; excessive cost and engineering effort required fabricate test articles prevented investigation in this work. Of other concern is the generally lower cycle life of hydroformed vs. edge-welded metal bellows. The nested convolute geometry may also be of potential interest for thermoplastic bellows formed by alternative methods to the typical high-travel PTFE bellows (lathe turning), such as blow and rotational molding and spray coating, as this may be more economical for larger parts with thin walls.

B. Potential Coating Failure Modes

We have identified several coating failure modes of interest on edge-welded bellows. In general, coatings may be cracked or otherwise lose their barrier properties in the bulk, or coating adhesion may be lost, resulting in separation from the metal substrate. The effects of cyclic straining (in-plane) in the bulk of the parylene film and at the parylene-metal interface due to flexing of the bellows during compression and extension are of concern. This may result in fatigue-based degradation in the bulk of the parylene film or loss of film adhesion. Ambient pressure cycling may have further deleterious effects. Cyclic contact between adjacent diaphragms (and associated out-of-plane strain) may cause damage; this might be reduced if bellows cycle distance is limited with a mechanical stop. However, we

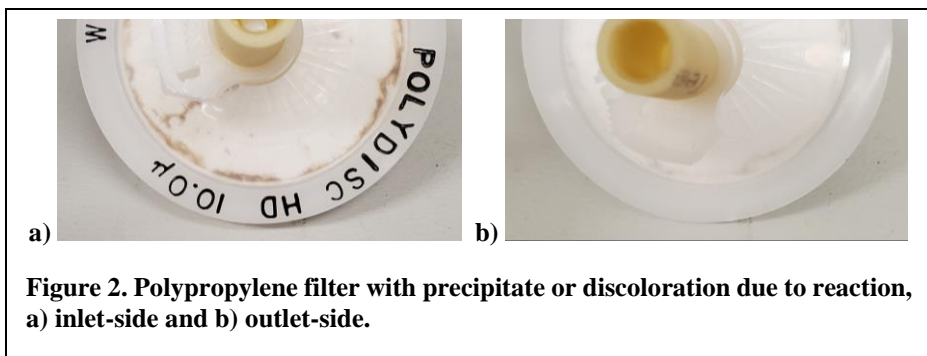


Figure 2. Polypropylene filter with precipitate or discoloration due to reaction, a) inlet-side and b) outlet-side.

hypothesize that the most significant degradation of the parylene coating may likely occur at/near the edge welds. This is due to possibility of high compressive stress and possible coating pulverization as well as crack initiation and growth (due to geometric stress concentration) towards the weld tip. It may be the case that the relatively small areas of exposed metal due to film damage at this location may become partially saturated with Ag-bearing deposits, as observed elsewhere,⁴ and diffusion rates may limit Ag⁺ transport from the bulk. This may result in reduced loss rates over time. The prospects for these must be verified experimentally, and small defects have the potential to result in significant local and bulk Ag⁺ depletion.

C. General System Description

The Bellows Testbed system consists of the following main subsystems: the bellows tank, the electro-pneumatic drive, the electronic timer/counter, and a digital data recorder with associated sensors. These are combined to enable automated long duration cycling of the bellows for Ag⁺ loss experiments. Schematics of the testbed system and the bellows tank, and a photograph of the electro-pneumatic drive are reproduced in Figures. 3a-c, respectively. The main structural-elements are made with stainless steel tri-clamp sanitary spools and end fittings. The bellows tank is constructed from an edge-welded metal bellows and associated hardware, such as the surrounding pressure vessel, a secondary water reservoir, a mechanical guide/stop assembly, and position sensor. The electro-pneumatic drive system is used to modulate the air pressures at the wet and dry sides of the bellows tank, using a three-way solenoid valve connected to a pressure-regulated source and backpressure-regulated vent.

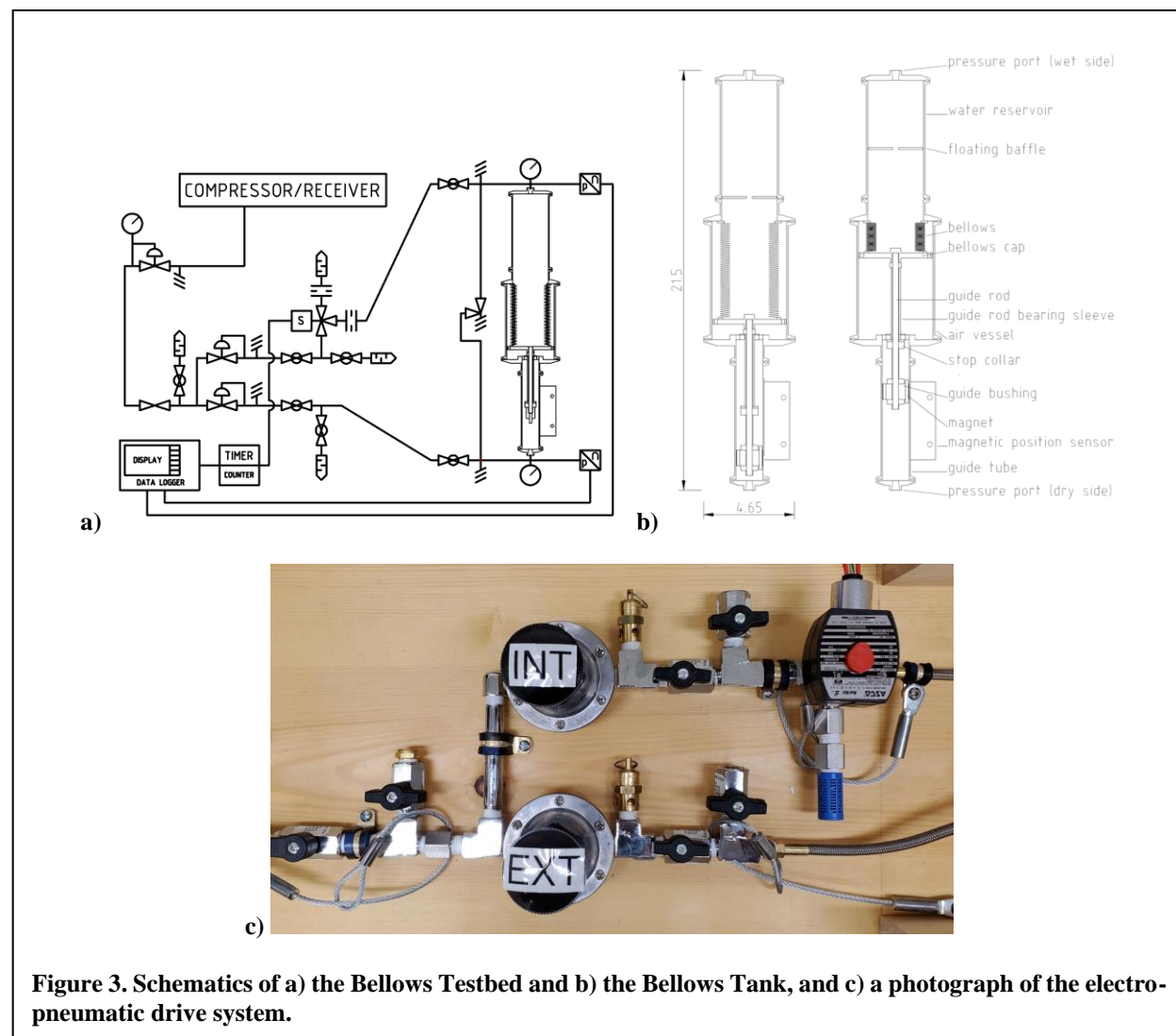


Figure 3. Schematics of a) the Bellows Testbed and b) the Bellows Tank, and c) a photograph of the electro-pneumatic drive system.

tank and electro-pneumatic drive are described in greater detail below. The electronic timer/counter has a relay output that is used to control the three-way solenoid valve of the electro-pneumatic drive. The cycle time and duty cycle can be selected to adjust the frequency of bellows motion, and to select what fraction of time the bellow is in the extended or compressed state. The speed of bellows motion can be adjusted by changing the size of a flow-restricting orifice in the electro-pneumatic drive system. The counter controls the number of bellows cycles in a given experiment. The digital data recorder is connected to pressure transducers at the pressure ports on the wet and dry sides of the bellows tank, and a linear position sensor detects the position of a magnet mounted in the guide bushing (through the stainless steel guide tube). This suite of sensors allows for mapping of bellows extension vs. differential pressure, real-time system monitoring and display of sensor readings, and post-experiment verification of bellows cycling.

D. The Bellows Tank

The Bellows Tank (Figures 3b, and 4a) consists of the Bellows Assembly (Figure 4b), a surrounding pressure vessel, a secondary water reservoir attached to the open end of the bellows assembly, an adjustable mechanical stop to limit bellows travel during cycling, and associated hardware that maintains bellows alignment. When the bellows is compressed, the Ag^+ solution flows upwards into the liquid reservoir. The wetted surfaces of the bellows tank are to be coated with a 25 μm (nominal) parylene-C coating with AdPro Plus adhesion promoter.

The Bellows Assembly consists of an edge-welded bellows and attached end fittings. The bellows was designed by Duraflex Inc. of Illinois. The bellows has an internal diameter of 2.75" (70 mm), outer diameter of 3.50" (89 mm), free length of ~3.25" (83 mm), and a convolution pitch (see Figure 4c) of approximately 0.10" (2.5 mm) at free length. It is constructed of three-ripple diaphragms with flats near the welds (Duraflex, Inc. die #A0350) stamped out of 0.005" (0.127 mm) annealed and passivated 316L stainless steel. A cross section showing the diaphragm geometry is reproduced in Fig. 4c. The diaphragms are stacked and welded at their internal and external diameters under argon shielding gas to prevent surface oxidation or contamination of the weld. The bellows can be compressed to roughly 30% of its free length, requiring a differential pressure of approximately 4.7 psi (32 kPa). Claimed cycle life is at least 35,000. This geometry was chosen because it was the most representative to that of the larger bellows employed on the ISS that was commercially available in a diameter practical for early stage laboratory testing, particularly with regards to the ratio of diaphragm outer diameter to span (O.D.-I.D./2, shown in Figure 4c). This ratio is generally higher with larger bellows, and the A0350 has the highest (most representative of the ISS bellows O.D./span ratio we found in standard designs by the manufacturers investigated without going to much larger diameters that would be impractical for initial sub-scale experiments. The convolution pitch is about 0.1 inch, which is believed to be ~1.5/2 times less than that of the larger ISS bellows, however the span/pitch ratio should be representative due to the small span of this bellows.

A deposition fixture, shown in Figure 4d, was designed and fabricated to allow parylene-C deposition with the bellows extended beyond their normal full extension, to allow greater penetration into the convolutions where the bellows diaphragms meet.

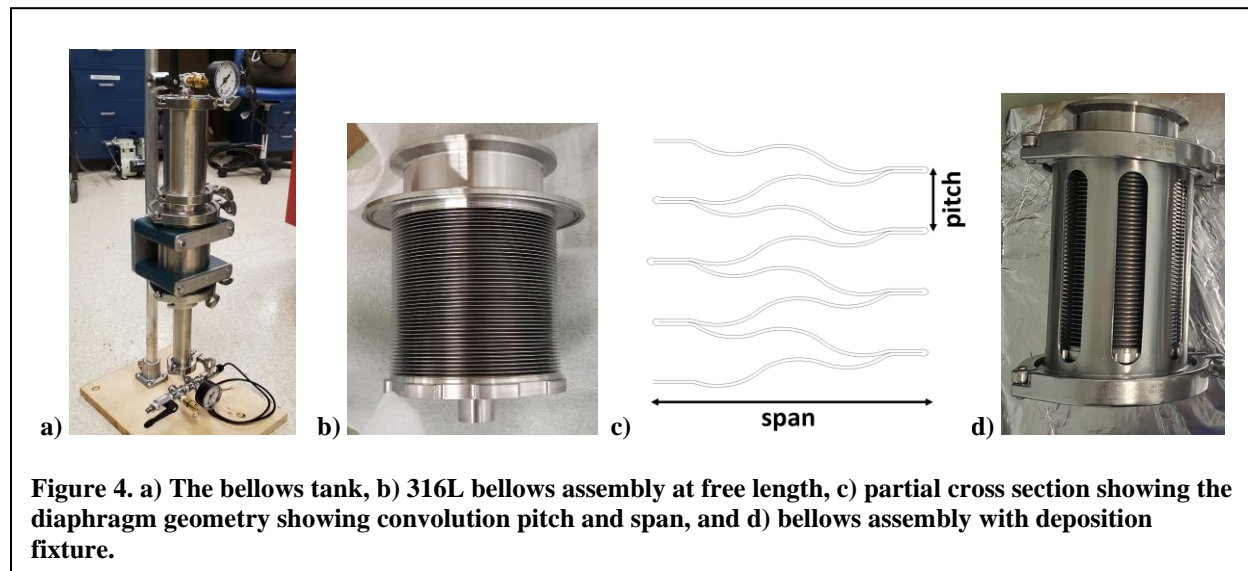


Figure 4. a) The bellows tank, b) 316L bellows assembly at free length, c) partial cross section showing the diaphragm geometry showing convolution pitch and span, and d) bellows assembly with deposition fixture.

E. The Electro-Pneumatic Drive

The electro-pneumatic drive system was designed to provide controlled compression and extension of the bellows by varying the pressure across the bellows. A regulated pressure source for the wet (water-containing) side of the bellows is alternately pressurized and vented to the atmosphere with a three-way solenoid valve (ASCO part # EF8320G20024/DCDD). The dry side of the bellows is kept at a near-constant, positive pressure vs. ambient. The pressure regulators selected were ITT Conoflow model GH10, 0-15 psi (0-100 kPa) service pressure (wet side: part # GH10XTHMAXAB, non-pressure relieving, and dry side: part # CGH10XTHEAXAB, pressure relieving). A schematic of the modified drive system is shown in Figure 3a, and an image of the hardware is shown in Figure 3c.

F. Preliminary Operation and Function Checks

Operation of the bellows tank with the updated electro-pneumatic drive system and an uncoated bellows has been confirmed, along with successful recording of the differential pressure and bellows position vs. time during the bellows expansion/compression cycle. We are waiting on the permanent installation of a clean compressed air source to begin experiments.

IV. Parylene-C Performance with Tube/Fitting Systems

A. Experimental Materials and Methods

6" (150 mm) long tubes were fabricated from 1/2" (12.7 mm) diameter seamless ultra-high purity 316L tubing (Swagelok). The tubing had a wall thickness of 0.049" (1.2 mm) and an electropolished internal surface with 0.25 μm average roughness. 316L Swagelok VCO™ Weld Glands were TIG welded to one end of the tubes. These were then pickled¹² and passivated¹³ to remove any heat tint or scale on the interior of the tube. Another set of tubes from the same tubing stock was flared manually on one end with a 37° AN flaring tool. The flare connections were then set by the torque method (described below) on 316L plugs (McMaster-Carr) and then disassembled for parylene coating. A set of 6" (150 mm) long tubes with a 1/2" (nominal size) tri-clamp ferrule on one end were made by cutting 12" (300 mm) long 316L sanitary spools (O.D. = 0.50" (12.7 mm), I.D. = 0.37" (9.4 mm), McMaster-Carr) in half. The tube ends and caps/plugs of the three systems investigated are shown without seals in Figure 5.

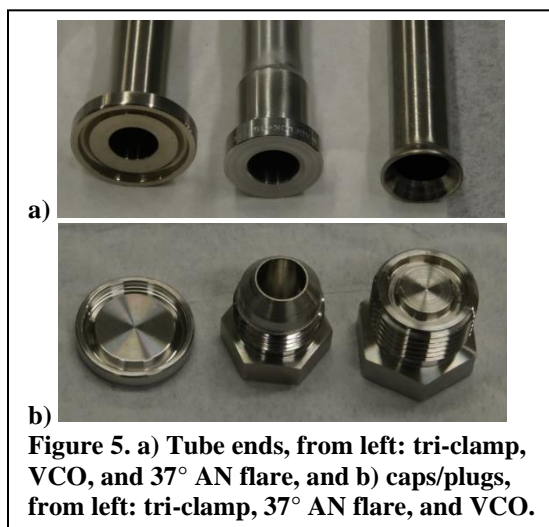


Figure 5. a) Tube ends, from left: tri-clamp, VCO, and 37° AN flare, and b) caps/plugs, from left: tri-clamp, 37° AN flare, and VCO.

The specimens were degreased with sequential hot water solutions of Dawn Detergent and Crystal Simple Green, rinsed with deionized water, and delivered to Specialty Coating Systems, Inc. (SCS, Clear Lake, WI). The samples were then rinsed in a deionized water/isopropyl alcohol solution and dried before being placed in the deposition chamber. A proprietary adhesion promoter, AdPro Plus™, was applied from the vapor phase *in situ* before parylene deposition. A 25 μm (nominal) coating of parylene-C was deposited on the tubes and associated end fittings (caps and plugs, not assembled). The threads on the 37° AN flare and Swagelok VCO™ end fittings were masked prior to deposition by SCS to allow for proper fitting assembly.

The tubes and associated fittings with caps or plugs were assembled prior to first filling with Ag^+ solution, and then disassembled and reassembled after each Ag^+ determination, prior to refilling with fresh solution. The experiments were done in quintuplicate. The VCO™ and tri-clamp fittings were assembled/disassembled one additional time before the first filling, as the desirability of pre-aging the Viton™ O-rings/gaskets was not known initially. The threads of the 37° AN plug were lubricated with an inert grease (Chemours Krytox GPL 205) to prevent galling while the AN nut was tightened to ~40 lb.-ft. (~54 N-m) using a torque wrench and crowfoot. The relative rotation of the tube and 37° AN plug was minimized with a fixturing device of our own design (Figure 6) in order to minimize damage of the parylene-C coating, which had been observed to be significant if free rotation was allowed.⁴ The Swagelok VCO™



Figure 6. The 37° AN flare fitting assembly fixture with tube and fitting.

fitting was assembled by hand-tightening the associated nut and then wrench-tightening a further 45°. The tri-clamp sanitary fitting was held together using a hinged clamp (with thumbnut) that was hand-tightened. The VCO™ O-rings and tri-clamp gaskets were ca. 70A durometer Viton™ rubber, and were pre-treated by extended exposure to ca. 400 ppb Ag⁺ solution to minimize Ag⁺ uptake in the experiments. No lubricant was used on the seals.

A solution with ca. 470 µg AgF and 735 µg NaF per 1,000 ml deionized water (containing ca. 400ppb Ag⁺, 400 ppb Na⁺, and 400 ppb F⁻) was made as described previously.² Each tube was filled with 6 ml of the Ag⁺ solution, with A/V ~ 4 cm⁻¹. The end fittings were then struck vertically and horizontally against a hard laboratory bench to dislodge air bubbles adhered to internal surfaces. Control samples were stored in inert polypropylene containers. Ag⁺ loss determination with an ion-selective electrode,² disassembly, reassembly, and refilling with fresh solution was done at 1, 2, 6, and 19 weeks with an ion-selective electrode. Macrophotography was done on the mating surfaces of the tubes and fitting caps/plugs prior to each assembly to record any visible damage to the parylene-C coating.

B. Experimental Results and Discussion

The results of the Ag⁺ loss determinations with the parylene-C coated tubes and fittings are shown in Table 1. All three fitting systems had minimal Ag⁺ loss at 1, 2, and 6 weeks, suggesting that a few assembly/disassembly cycles do not significantly reduce Ag⁺ loss mitigation performance. It is unclear at this point if the increased losses at 19 weeks for the VCO and sanitary fittings are due to coating damage or Ag⁺ uptake to the Viton seals over a longer time period. Cumulative damage and minute exposure of the bare metal in wetted areas, as is demonstrated by the increased losses at 19 weeks. Without pre-treatment, many elastomers show significant uptake at moderate A/V ratios.⁹ The 10% average loss at 19 weeks with the Tri-clamp samples is attributed in part to the Viton gasket employed as Viton shows slow “aging” or saturation, as reported later in this work. However, the pre-treatment of the Viton™ O-rings and gaskets used with the Swagelok VCO and Tri-clamp sanitary fittings is believed to have reduced Ag⁺ uptake by partial saturation of adsorption sites. The larger losses at 6 and 19 weeks with the Swagelok VCO™ fitting are believed to be due in part to hard contact between the fittings and visible damage to wetted areas of parylene-C on metal, discussed below. Interestingly, the 37° AN flare fitting samples showed superior performance through 19 weeks, even with visible damage to the coating, discussed below. This may be due to the component mating geometry of the fully-assembled fittings or poor wetting preventing significant exposure to the areas with damaged coating and the bare metal below. Longer duration testing is required to determine if the trend of increasing loss rate observed between 6 and 19 weeks, corresponding to exposure of bare metal, is maintained.

Macrographs of the Swagelok VCO™ and Tri-clamp sanitary fittings from before 19 weeks are not reproduced here, as no appreciable damage to the parylene-C coatings beyond minor blistering/substrate discoloration was visible. By 19 weeks, moderate blistering and substrate discoloration were visible in both cases, shown in Figures 7a and 7b. In the case of the tri-clamp fitting, the soft gasket appeared to have protected the parylene coating from damage (Figure

7a). In the case of the VCO™ fitting, there is a small annular section of hard contact between the two parylene-coated metal parts that is wetted. Delamination here is apparent in Figure 7c, visible by the whitening of the film. The relative contributions of the larger Ag⁺ loss recorded at 19

Table 1: Results of Experiments with Tubes/Fittings

Fitting:	Mean Ag ⁺ loss* [%]			
	Total time immersed [weeks]			
	1	2	6	19
<i>Tri-clamp (sanitary gasket)*</i>	6	5	4	10
<i>VCO Face-seal O-ring*</i>	6	5	9	22
<i>37° AN flare fitting</i>	5	3	1	7
<i>A/V~4 cm⁻¹. Disassembled, reassembled, and refilled with fresh 400 ppb Ag⁺ soln. after each determination. Performed in quintuplicate.</i>				
<i>*One disassembly/reassembly cycle before first immersion</i>				

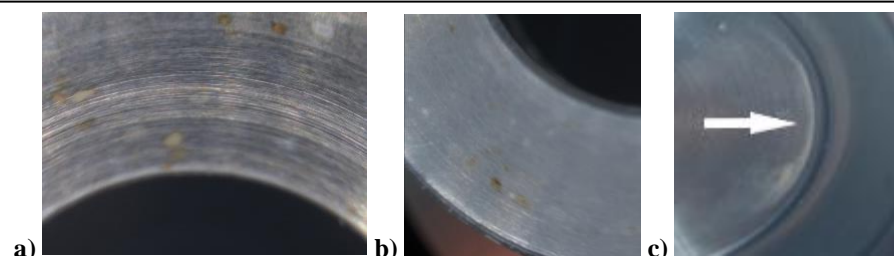


Figure 7. a) Tri-clamp ferrule, b) VCO tube gland, and c) VCO plug after 19 weeks immersion and five assembly/disassembly cycles (the white arrow points toward the damaged/delaminated area).

weeks to the Viton O-ring or metal potentially exposed by coating damage is unclear. A simple relief cut on the VCO fitting could be used to eliminate the hard contact between the two parylene-coated metal parts and the potential coating damage in a wetted location. In the case of the VCO fittings, the tube was allowed to rotate freely during final tightening of the fitting nut, but observed rotation was minimal due to the friction provided by the compressed O-ring seal.

Macrographs of the 37 deg, AN flared tubing and plug after 1-4 assembly/disassembly cycles (at 1, 2, 6, and 19 weeks) with our assembly fixture are shown in Figure 8. Coating damage, corresponding to the mating surfaces is visible, but even after four cycles this is visibly much less than one cycle where free relative rotation is allowed.⁴ It should be noted that a limited amount of the Krytox GPL 205 grease was transferred unintentionally from the plug/nut threads to the tip of the plug during disassembly. Although we attempted to clean the mating surfaces with paper laboratory wipes, some of the grease may have remained and potentially covered metal exposed by parylene-C coating damage. Deliberate use of such grease to protect mating surfaces may be a useful technique to minimize coating damage during assembly or cover small areas of exposed metal, as the perfluoropolyether-based lubricant is incidental food contact grade, highly-inert, and completely insoluble in water.

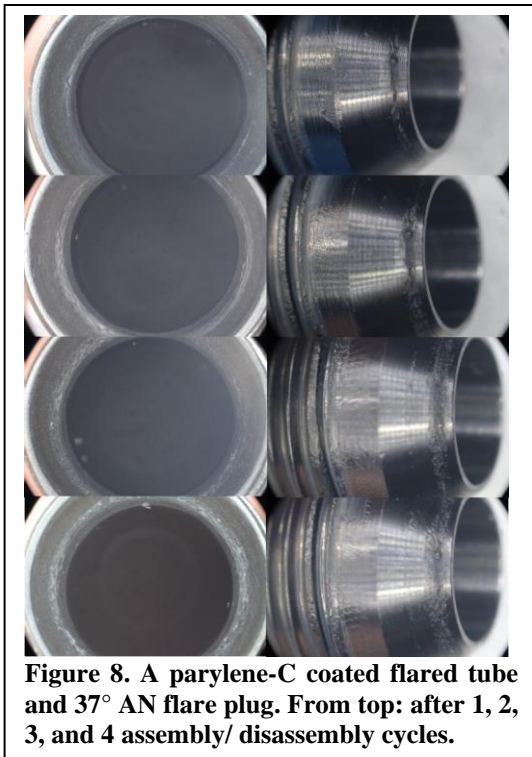


Figure 8. A parylene-C coated flared tube and 37° AN flare plug. From top: after 1, 2, 3, and 4 assembly/ disassembly cycles.

V. Ag^+ Compatibility with Seal Materials

A. Experimental Materials and Methods

The Ag^+ uptake and saturation behavior of Viton (fluorocarbon) and Kalrez (perfluorocarbon) seals were investigated, in order to determine compatible seal materials for potential use in potable water systems, and with parylene-coated tubes/fittings in particular. The Viton samples were made by cutting 60° sections from circular 3" tri-clamp sanitary gaskets. Gray Viton gaskets were purchased from Glacier Tanks, and black Viton gaskets from Austenitex. AS568 -111 size Kalrez O-rings in grade 6230 and 3/4" tri-clamp sanitary gaskets in grade 6230A (both FDA food contact grade) were manufactured by DuPont/Chemours. The samples were cleaned by rinsing/soaking in deionized water. A subset of the Viton (gray and black) samples were pre-treated by soaking in 100 ppm Ag^+ solution for three days and then rinsed three times in deionized water to remove labile Ag^+ . One cut section of the Viton gasket, three -111 Kalrez O-rings, and one 3/4" Kalrez gasket were placed in 6 ml of 400 ppb Ag^+ solution in 12 ml polypropylene tubes, resulting in A/V of 1.8, 1.7, and 1.3 cm^{-1} respectively. Ag^+ determination and refilling with fresh solution was done for the Viton samples at 1, 2, 3, 7, 14, 21, 28, and 148 (Glacier Tanks Gray Viton only) days, and for the Kalrez samples at 1, 2, and 4 weeks. Ag^+ solution make-up and loss determination was done as described in the previous section. The experiments were performed in triplicate for the Glacier Tanks gray Viton and Kalrez O-ring and gasket samples, and in duplicate for the Austenitex black Viton gaskets.

B. Experimental Results and Discussion

The results of the experiments with Viton gaskets is shown in Table 2. As was expected, given results from a previous work,⁹ significant Ag^+ uptake occurred during the first 7 days of immersion, with reduction in time-normalized loss rates as duration of exposure increases and adsorption sites become partially saturated. The Austenitex black Viton showed consistently lower losses than the Glacier Tanks gray Viton, likely due to differences in the compound, fillers, other additive materials, or the chemical or manufacturing process. A single outlier sample of the Glacier gray Viton was removed from the reported data as it consistently showed significantly larger losses, likely due to contamination or compositional variation. With the Glacier gray Viton, pre-treatment with 100 ppm Ag^+ resulted in a large initial release of Ag^+ and continuing reduced loss rates vs. the untreated samples. The much larger initial and continuing release of Ag^+ by the pre-treated Austenitex black Viton may also be potentially explained by

compositional or structural differences. However, by 28 days, release of excess adsorbed silver appears to have effectively stopped, and further long-term immersion could potentially result in large losses, as seen in the 148-day determination for the pre-treated Glacier Tanks gray Viton.

Table 2: Results of Experiments with Viton Seals

Material:	A/V [cm ⁻¹]	Mean Ag ⁺ loss [%]							
		Total time immersed [days]							
		1	2	3	7	14	21	28	148
<i>Glacier Tanks Gray Viton†</i>	1.8	25	14	10	11	9	9	10	44
<i>Glacier Tanks Gray Viton*</i>	1.8	-32§	-2§	11	-1§	-4§	2	6	33
<i>Austenitex Black Viton</i>	1.8	19	10	8	9	2	4	6	N/A
<i>Austenitex Black Viton*</i>	1.8	-225§	-115§	-63§	-80§	-42§	-20§	-3§	N/A
All refilled with fresh 400 ppb Ag ⁺ soln. after each determination.									
*Pre-treated with 100 ppm Ag ⁺ soln.									
†A single outlier was removed.									
§Ag ⁺ concentration increased.									

The results of the experiments with Kalrez O-rings and gaskets is shown in Table 3. The much larger loss for the 6230A grade gaskets vs the 6230 grade O-rings could potentially be due to slight differences in composition or the use of a reactive mold-release compound, but behavior became similar by the second determination. Both materials showed significantly smaller cumulative Ag⁺ uptake after a given duration of immersion than the Viton materials investigated here, but these limited results unfortunately provide limited insight into the saturation or “aging behavior” of Kalrez. These results are consistent with previous 1-week tests⁹ with Viton and Kalrez (done with A/V of 2 cm⁻¹), which found essentially no loss for Kalrez and near total loss for Viton. In those experiments, a different grade of Kalrez was used, 4079,¹⁴ which may have superior Ag⁺ compatibility to the 6230/6230A grades used here, although the single immersion period used in that study and the small losses observed here prevent definite conclusions. Future work is necessary to determine if high-concentration pre-treatment or further aging with 400 ppb Ag⁺ can effectively saturate Kalrez and allow for minimal loss during long periods of system dormancy. However, these preliminary results show Kalrez to be one of the more promising elastomers with respect to Ag⁺ compatibility, with the downside of significantly elevated cost and limited COTS availability in seal products vs. Viton and other commodity grade materials.

Table 3: Results of Experiments with Kalrez Seals

Material:	A/V [cm ⁻¹]	Mean Ag ⁺ loss [%]		
		Total time immersed [weeks]		
		1	2	4
<i>Kalrez 6230 -111 O-rings (×3)</i>	1.7	4	5	10
<i>Kalrez 6230A 3/4" sanitary gasket (×1)</i>	1.3	21	6	8
All refilled with fresh 400 ppb Ag ⁺ soln. after each determination.				

While the Ag⁺ uptake and “aging” behavior of elastomers⁹ appears significantly worse than many rigid thermoplastics^{1,9} and parylene,^{2,4} this may not preclude their limited use in seals, where wetted area is minimal. Alternative seal designs, including gaskets and O-rings with more inert (PTFE or FEP) encapsulation are also available, although these harder materials have greater potential to damage soft coatings such as parylene during seal installation and fitting assembly. Further work is necessary to identify elastomers and associated pre-treatments suitable for large wetted area components, such as the relatively thick bladders often used in positive expulsion tanks.

VI. Future Work

Operation of the two testbed systems described here will begin in the near future. Once parylene-C performance has been characterized, other promising barrier coatings, including thin-film ceramics, could be investigated in follow-up work. We plan on continuing the experiments concerning tube fitting compatibility with parylene-C barrier coatings to investigate performance after long-term water exposure. Minor modifications to standard/COTS fitting systems

could reduce coating damage and should be investigated. The effects of barrier coatings, including potential defects, on fitting leak rate, along with the relative performance of fittings that rely on metal-metal (hard) and elastomer (soft) seals should be considered. Further effort is necessary to identify Ag⁺ compatible elastomers for seals and other flexible components, and to characterize the effects of “aging” and high-concentration pre-treatment. We also intend to continue long-term Ag⁺ loss and adhesion experiments with parylene-coated that have been ongoing from our earlier work.

VII. Conclusions

In previous reports, we have described our results characterizing the Ag⁺ loss mitigation and adhesion performance of parylene barrier coatings on several metal alloys with various surface treatments and structures. In this work, we described the motivation, construction, and operational principles of the two testbed systems that were developed to characterize parylene-C performance under more realistic mechanical challenges. The Flow/Pressure Testbed will provide flow and pressure cycling to probe coating performance with internally-coated 316L tubing. The mechanical operation of the Flow/Pressure Testbed has been confirmed, however the cause of excessive Ag⁺ loss during control experiments has yet to be identified and mitigated. The Bellows Testbed provides cycling operation of a 316L edge-welded bellows tank, suitable as a sub-scale analog for the bellows tanks used for potable water storage and delivery on the ISS. All operational functions of the Bellows Testbed have been confirmed, and experiments will commence after a permanent source of compressed air has been installed.

We completed medium-duration experiments with parylene-C coatings on 316L tubing, investigating three fitting systems: Tri-clamp sanitary gasket, Swagelok VCO face O-ring seal, and 37°AN flare fittings. These all were found to be compatible with multiple assembly/disassembly cycles, but coating damage was observed in some cases. We showed that pre-treatment of Viton with high-concentration Ag⁺ or “aging” at biocidal concentrations can significantly reduce Ag⁺ uptake rates. We confirmed that Kalrez has superior Ag⁺ compatibility than that of Viton.

Acknowledgments

The authors would like to thank Duraflex, Inc. for helpful conversations regarding the design and function of edge-welded bellows and John Steele for information regarding the ISS WPA and Potable Water Storage and Delivery ORUs. We acknowledge the Advanced Exploration Systems – Habitation Systems Project for financial support.

References

- ¹Vance, J., Shaw, A., and Delzeit, D., “Engineering Polymers as Structural Materials in Spacecraft Water Systems,” *51st International Conference on Environmental Systems*, ICES-2022-7, 10-14 July 2022, Saint Paul, Minnesota. (In review)
- ²Vance, J. and Delzeit, L., “Mitigation of Silver Ion Loss from Solution by Polymer Coating of Metal Surfaces,” *49th International Conference on Environmental Systems*, ICES-2019-125, 7-11 July 2019, Boston, Massachusetts.
- ³Vance, J. and Delzeit, L., “Mitigation of Silver Ion Loss from Solution by Polymer Coating of Metal Surfaces, Part II,” *50th International Conference on Environmental Systems*, ICES-2020-22.
- ⁴Vance, J. and Delzeit, L., “Mitigation of Silver Ion Loss from Solution by Polymer Coating of Metal Surfaces, Part III,” *50th International Conference on Environmental Systems*, ICES-2021-30, (virtual).
- ⁵Vance, J. and Delzeit, L., “Characterization of Parylene Coatings and Testbed Development: FY2020 Final Report,” Report to NASA Advanced Exploration Systems Management, 2020.
- ⁶Vance, J. and Delzeit, L., “Characterization of Parylene Coatings and Testbed Development: AgLoss FY2021 Final Report,” Report to NASA Advanced Exploration Systems Management, 2021.
- ⁷Maryatt, B., “Lessons Learned for the International Space Station Potable Water Dispenser,” *48th International Conference on Environmental Systems*, ICES-2018, 8-12 July 2018, Albuquerque, New Mexico.
- ⁸Steele, J., Personal Communication, January 16, 2020.
- ⁹Colón-Colón, H., Button-Denby, A., Steele, J., and Nelson, J., “Early Results from a Broad Compatibility Study of Various Materials with Ionic Silver Biocide,” *50th International Conference on Environmental Systems*, ICES-2020-476.
- ¹⁰Steele, J., Personal Communication, January 20, 2020.
- ¹¹Gardner, R. I., U.S. Patent 3,469,502, 1969.
- ¹²ASTM A380/A380M-17, Standard Practice for Cleaning, Descaling, and Passivation of Stainless Steel Parts, Equipment, and Systems, ASTM International, West Conshohocken, PA, 2017.

¹³ASTM A967/A967M-17, Standard Specification for Chemical Passivation Treatments for Stainless Steel Parts, ASTM International, West Conshohocken, PA, 2017.

¹⁴Colón-Colón, H., Personal Communication, March 19, 2020.